Journal of Materials Science & Technology 43 (2020) 14–20

Contents lists available at ScienceDirect

Journal of Materials Science & Technology

journal homepage: www.jmst.org

Research Article

Inhibition effects of benzalkonium chloride on *Chlorella vulgaris* induced corrosion of carbon steel

Junlei Wang[a,b], Tiansui Zhang[a], Xinxin Zhang[a], Muhammed Asif[a], Lipei Jiang[a], Shuang Dong[c], Tingyue Gu[b], Hongfang Liu[a,*]

[a] School of Chemistry and Chemical Engineering, Huazhong University of Science and Technology, Wuhan, Hubei, 430074, China
[b] Department of Chemical and Biomolecular Engineering, Institute for Corrosion and Multiphase Technology, Ohio University, Athens, OH, 45701, USA
[c] School of Chemical Engineering and Materials, Changzhou Institute of Technology, Changzhou, Jiangsu, 213032, China

ARTICLE INFO

Article history:
Received 16 June 2019
Received in revised form
16 September 2019
Accepted 19 September 2019
Available online 7 January 2020

Keywords:
Benzalkonium chloride
Chlorella vulgaris
Carbon steel
Corrosion
Electrochemistry

ABSTRACT

In this work, a surfactant, benzalkonium chloride (BAC), was used to study its effects on both the growth of *Chlorella vulgaris* and the corrosion caused by its biofilm. Experimental results indicated that BAC at a low concentration of 3 mg/L suppressed *C. vulgaris* growth and achieved 81% corrosion inhibition based on weight loss reduction. The inhibition effects increased when the BAC dosage was increased. At 30 mg/L, the corrosion inhibition increased to 95%. Electrochemical results supported surface pitting analysis, weight loss results data and confirmed the corrosion inhibition.

1. Introduction

Carbon steels are widely used in various industries, with applications in vessels, bridges, buildings and so on. However, carbon steels are easily corroded in harsh environments leading to costly economic losses each year [1–6]. Hence, it is crucial to study the corrosion behavior of carbon steel and take measures to decrease the corrosion. Microbiologically influenced corrosion (MIC) is the corrosion caused or accelerated by the metabolic activities or products of microorganisms. It accounts for 20% of all corrosion losses [7].

Microorganisms can participate in the failure process of metal materials [8–19]. Among corrosive microorganisms, sulfate reducing bacteria (SRB), iron oxidizing bacteria and nitrate reducing bacteria have been investigated systematically in recent years [9,11,20–23]. MIC caused by fungi has also drawn serious attention. Behaviors of fungal MIC of metal substrates have been evaluated by researchers [12,13,24].

Algal MIC on materials degradation and its mitigation, however, has not been paid enough attention by researchers [25,26]. Algae are photosynthetic eukaryotic organisms that are widely present in recirculating water treatment systems and cooling water systems, ponds and lakes. Algae blooms occur due to water eutrophication and it is an important problem affecting water quality globally [27–29]. *Chlorella vulgaris* is a micro-alga, which has a rapid growth rate given a nutritionally adequate medium with abundant sunlight [30,31]. The metabolic activities/products of *C. vulgaris* can cause metal corrosion and thus decreases the service life of metal materials according to previous research [26,32]. Therefore, it is important to study biocide mitigation of *C. vulgaris* MIC of a metal substrate.

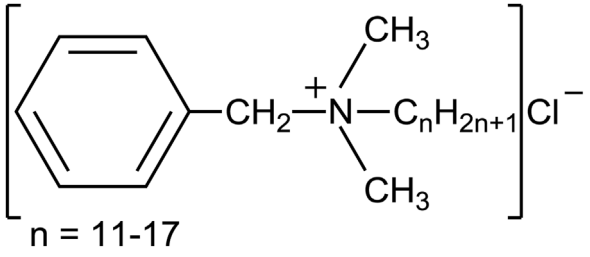

Fig. 1. Molecular structure of benzalkonium chloride (BAC).

Benzalkonium chloride (BAC) is a surfactant which is a cationic quaternary ammonium salt. It molecular structure is displayed in Fig. 1. BAC is used as an ingredient in cosmetics, a preservative in

* Corresponding author.
E-mail address: liuhf@hust.edu.cn (H. Liu).

https://doi.org/10.1016/j.jmst.2020.01.012
1005-0302/

medicines, a disinfectant in health care facilities and in hand sanitizers because it is regarded as safe for cleaning various surfaces [33,34]. BAC has a good abiotic corrosion inhibition ability on steels in a harsh environment possibly due to its adsorption on steel surface [35–38]. It has been proven that BAC at a concentration at or above 40 mg/L (40 ppm) inhibits SRB MIC of a carbon steel very well [39]. However, the dosage and efficacy of BAC against algal MIC are still unknown.

In this work, *C. vulgaris* MIC of a carbon steel and its inhibition by BAC was investigated. Electrochemical corrosion measurements, surface morphology and weight loss data were used to investigate the dosage and efficacy of BAC.

2. Experimental

2.1. Coupon preparation

The mass percentages of elementals in carbon steel X80 was: 0.07 C, 1.82 Mn, 0.056 Nb, 0.028 Al, 0.19 Si, 0.012 Ti, 0.007 P, 0.026 Cr, 0.02 Cu, 0.01 Mo, 0.17 Ni, 0.0001 B, 0.002V, 0.004N, 0.023 S and balance Fe. Coin-shaped specimens with an exposed area of 0.785 cm^2 were employed for weight loss tests and surface morphology observations. A cylinder-shaped specimen was welded with a copper wire, then sealed with epoxy resin with an exposed surface of 0.785 cm^2 (another plane) for electrochemical measurements. Prior to use, all specimens were polished using 180, 600, 1000 and 1200 grit Emery papers, then degreased and dehydrated with anhydrous acetone and alcohol, respectively. Finally, they were dried using a N_2 gas stream and sterilized under a UV lamp.

2.2. Microbe cultivation

C. vulgaris was separated from a water sample taken from East Lake, Wuhan, China. It was cultivated under laboratory conditions in open air at 25–30 °C with indirect natural sunlight during daytime and no lighting during nighttime. The planktonic algal growth characteristics have been reported in a previous work [26]. The composition of the culture medium contained (g/L): 0.0116 $CaCl_2{\cdot}2H_2O$, 0.24 K_2HPO_4, 0.0153 KH_2PO_4, 0.2 $MgSO_4$, and 0.5 carbamide. Before cultivation, the culture medium was sterilized in an autoclave at 121 °C for 20 min. After that, when the medium cooled to room temperature, it was inoculated with 10% (v/v) seed culture.

2.3. Weight loss measurements

After 14 days of incubation, Clarke's solution was used to remove biofilms and corrosion products from coupons [40]. After that, they were rinsed with distilled water, anhydrous ethyl alcohol and then dried under a nitrogen gas stream. The carbon steel corrosion rate was calculated based on coupon weight loss from the following equation [41,42]:

$$CR = \frac{87600\Delta m}{\rho \cdot S \cdot t} \quad (1)$$

where CR is the corrosion rate (mm/y), t the immersion time (h), Δm the weight loss of specimen (g), ρ density of carbon steel (g/cm^3) and S the exposed area of the coupon (cm^2).

2.4. Surface observation

A light microscope (VHX-1000E, Keyence, Japan) was used to observe algal cells on coupons at 200X magnification. The morphologies of corrosion products and biofilms were observed under scanning electron microscope (SEM) (Quanta 200, FEI, Netherlands). The coupons were retrieved from the culture medium after incubation and then the biofilms were using a phosphate buffered saline (PBS) solution (pH 7) containing 2.5% (v/v) glutaraldehyde for 4 h. After biofilm fixing, the coupons were immersed in a series of more concentrated ethyl alcohol concentrations to dehydrate before they were stored in a desiccator prior to use [26,43]. The corrosion morphology after removing the corrosion products and biofilms were examined under the 3D stereoscopic microscope (VHX-1000E).

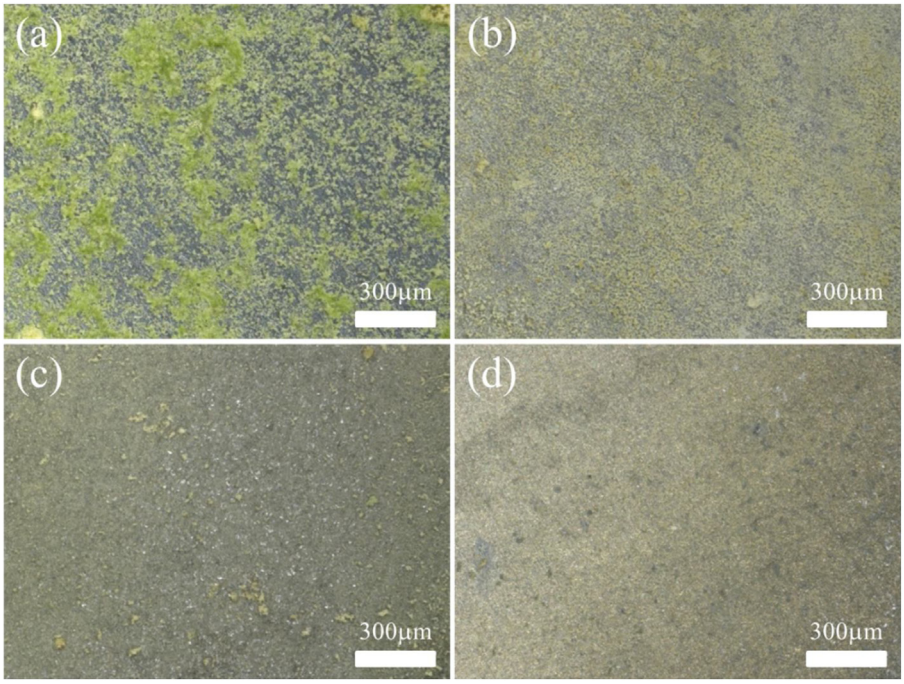

Fig. 2. Surface images of biofilm-covered coupons under light microscope at 200X after 5-day incubation for different BAC concentrations: (a) 0 mg/L, (b) 3 mg/L, (c) 10 mg/L, (d) 30 mg/L.

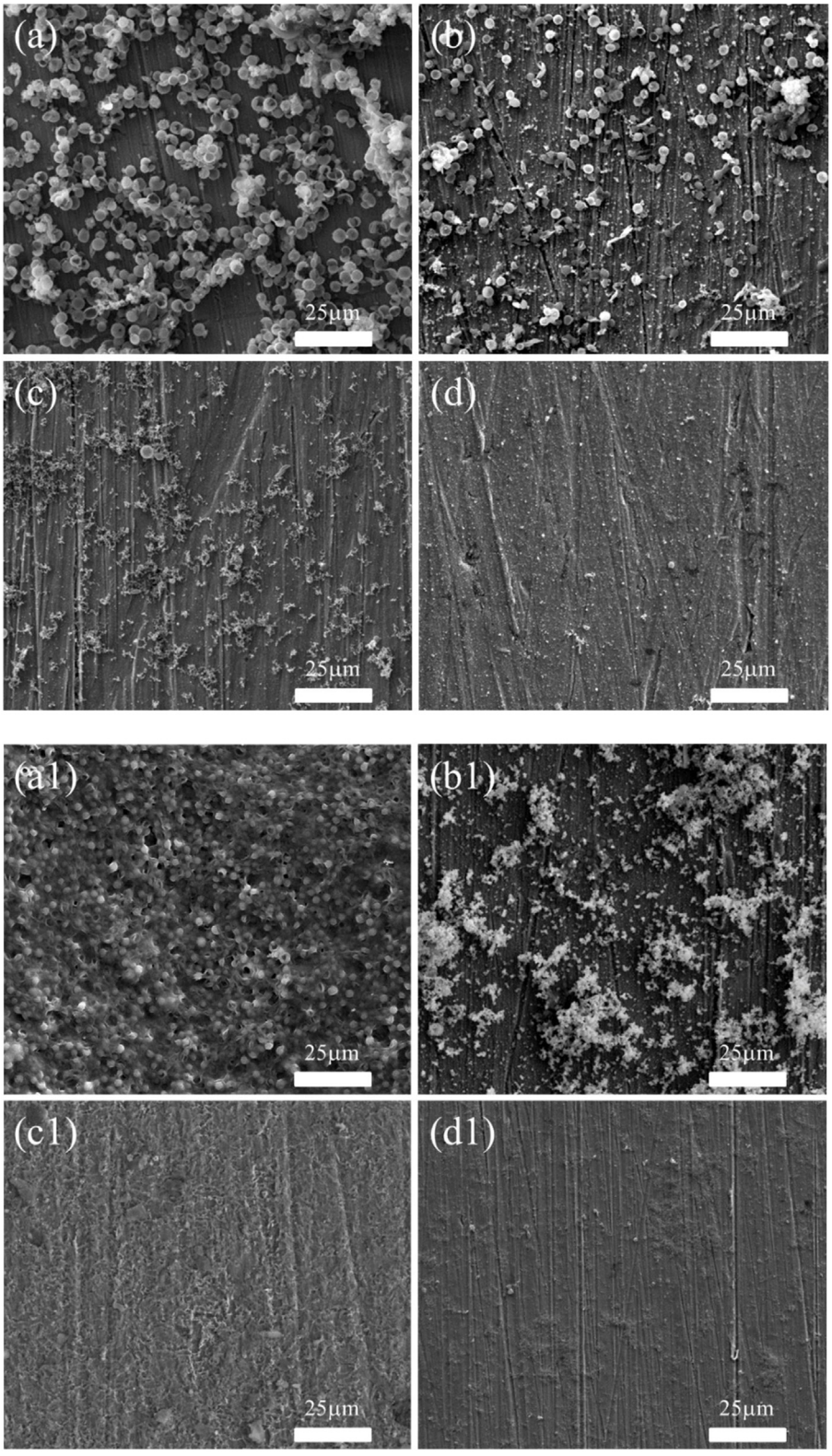

Fig. 3. SEM images of coupon surfaces after 5 days (a–d) and 14 days (a1-d1) of incubation for different BAC concentrations: (a, a1) 0 mg/L, (b, b1) 3 mg/L, (c, c1) 10 mg/L, (d, d1) 30 mg/L.

2.5. Electrochemical measurements

A three-electrode system was built to measure the electrochemical corrosion data. A saturated calomel electrode (SCE) and a platinum sheet were used as the reference and counter electrode, respectively. Each electrochemical glass cell was filled with 400 mL culture medium. Electrochemical impedance spectroscopy (EIS) was measured by applying a sinusoidal potential

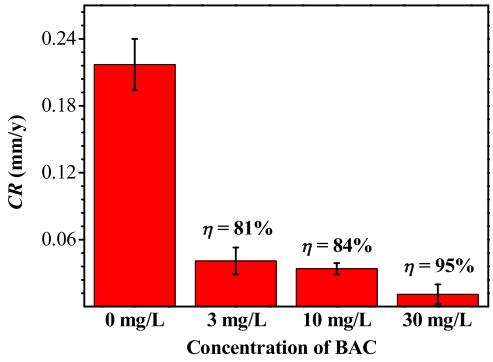

Fig. 4. Weight loss-based corrosion rates and corrosion inhibition efficiencies after 14 days of incubation for different BAC concentrations.

of 10 mV amplitude from the range of 10^{-2} to10^{5} Hz. EIS data were fitted using Zview software [12,44]. Potentiodynamic polarizations were scanned from −200 mV to 200 mV vs. open circuit potential (OCP) at the end of incubation. The results were fitted using Cview software for Tafel analysis [13,45].

3. Results and discussion

3.1. Biofilm morphology

Fig. 2 shows the optical images of specimens after 5 days of incubation. Clearly, in the absence of BAC, *C. vulgaris* formed a healthy biofilm on the carbon steel coupon (Fig. 2(a)). The sessile cell density was found to be 1.8×10^6 cells/cm^2 using a hemocytometer. BAC at 3 mg/L inhibited the sessile growth of *C. vulgaris* and reduced the sessile cell count to 5.3×10^4 cells/cm^2. Fig. 2 shows that higher BAC concentration (10 mg/L and 30 mg/L) inhibited growth further. The probable biocidal mechanism of BAC against the cells has been illustrated in the literature, suggesting that a positively charged atom of nitrogen in BAC could adsorb and then penetrate into a cell wall, leading to a membrane disruption [33].

3.2. SEM observation

SEM morphologies of specimens after 5 and 14 days of incubation are shown in Fig. 3. After 5 days and 14 days of incubation in the absence of BAC, well-defined bead-shaped sessile cells are abundant (Fig. 3(a)). With a low dosage of 3 mg/L, BAC significantly reduced the number of sessile cells. Increasing the dosage to 10 mg/L reduced the number of sessile cells further after 5 days of incubation and after 14 days of incubation, hardly any sessile cells are seen in Fig. 3(c1.). With a high dosage of 30 mg/L, only a few sessile cells remained (Fig. 3(d1)) after 5 days and after 14 days, virtually none stayed on the coupon surface which showed pristine polishing lines are visible in (Fig. 3(d1)).

3.3. Weight loss

Corrosion rates in the presence of *C. vulgaris* after 14 days of incubation with different BAC concentrations are shown in Fig. 4. The corrosion rate without BAC was quite largest (0.217 ± 0.023) mm/y because *C. vulgaris* acceleration of the corrosion process was not inhibited [26,32]. In comparison, in the presence of BAC, the corrosion rates were (0.041 ± 0.012) mm/y (3 mg/L BAC), (0.034 ± 0.005) mm/y (10 mg/L BAC) and (0.011 ± 0.009) mm/y (30 mg/L BAC). These data clearly indicate that BAC was effective in the mitigation of *C. vulgaris* MIC, with weight loss-based corrosion efficiencies of 81%, 84% and 95% for BAC concentrations of 3 mg/L, 10 mg/L and 30 mg/L, respectively.

3.4. D pitted surface morphology

After 14 days of incubation, 3D morphologies of coupon surfaces after removing biofilms and corrosion products were observed under the 3D stereoscopic microscope. Fig. 5 shows the surface roughness profiles for different BAC concentrations. The 3D surface profile (Fig. 5(a)) without BAC is shown elsewhere (Fig. S1). Judging from the scale bars, it is easy to see that with an increasing BAC concentration, the coupon surface became progressively smoother. The surface roughness decreased in the following order: 62.3 μm (0 mg/L BAC), 38.7 μm (3 mg/L BAC), 24.3 μm (10 mg/L BAC) and 17.0 μm (30 mg/L BAC).

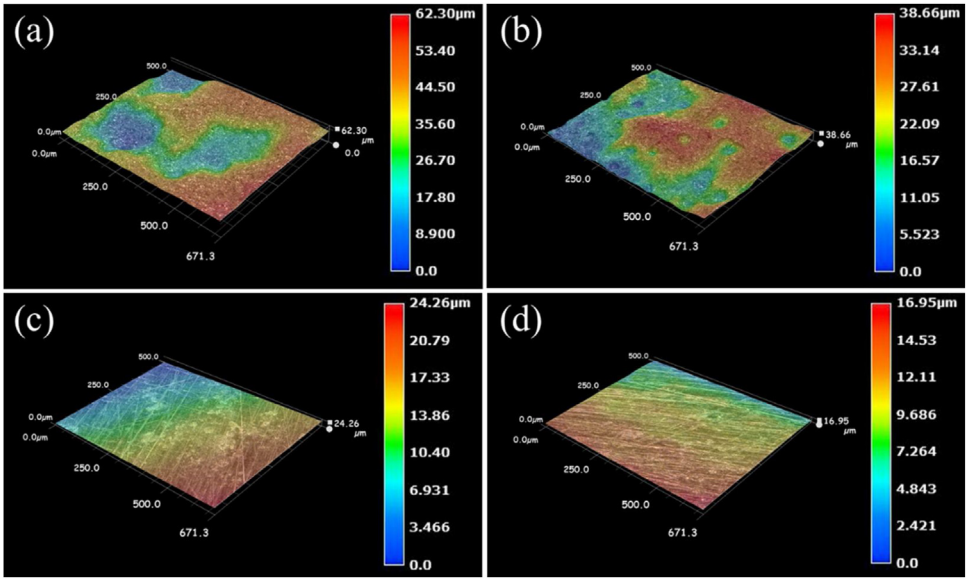

Fig. 5. 3D morphology of coupon surfaces with biofilms and corrosion products removed after 14 days of incubation for different BAC concentrations: (a) 0 mg/L, (b) 3 mg/L, (c) 10 mg/L, (d) 30 mg/L.

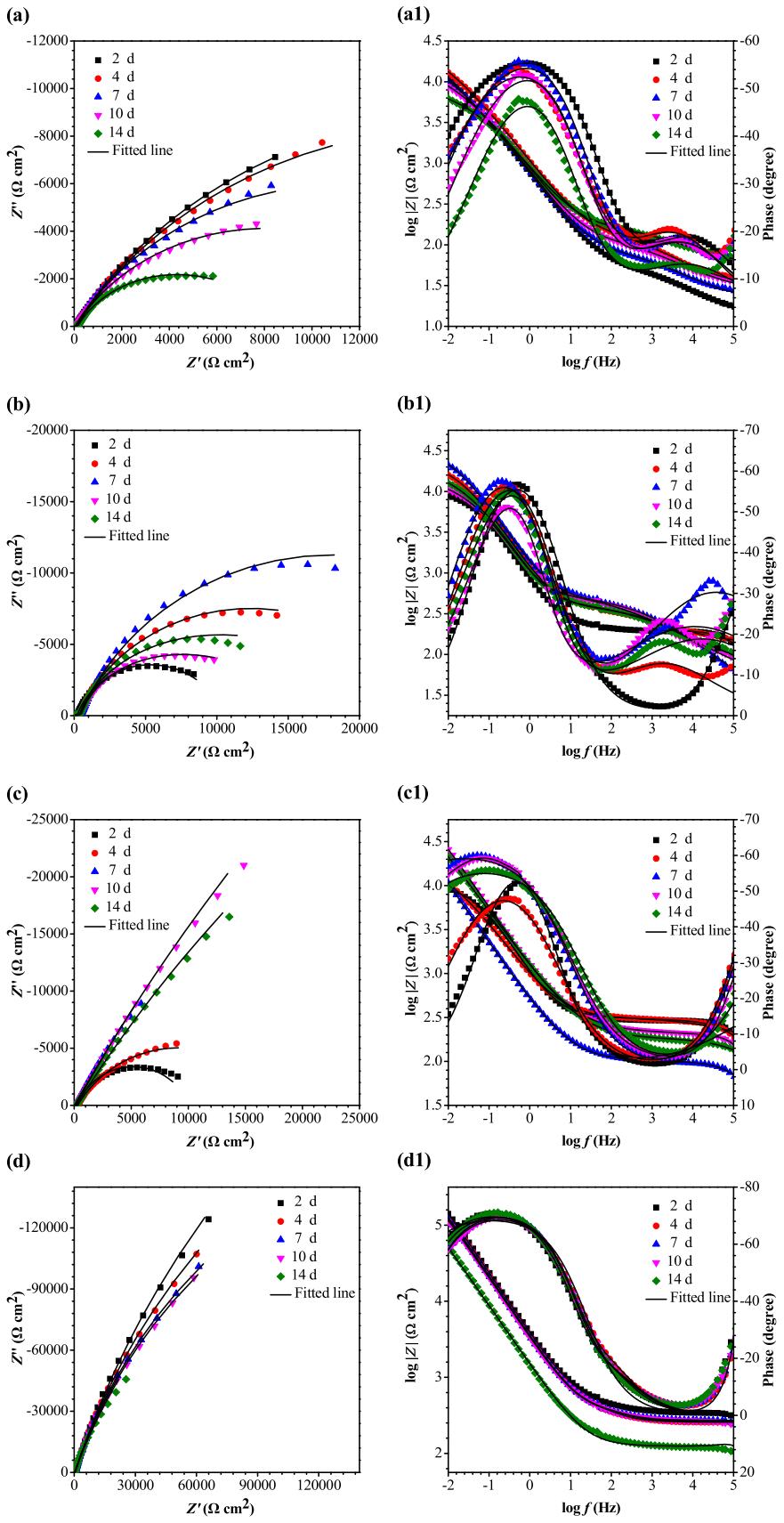

Fig. 6. Nyquist and Bode plots for different BAC concentrations in electrochemical glass cells: (a, a1) 0 mg/L, (b, b1) 3 mg/L, (c, c1) 10 mg/L, (d, d1) 30 mg/L.

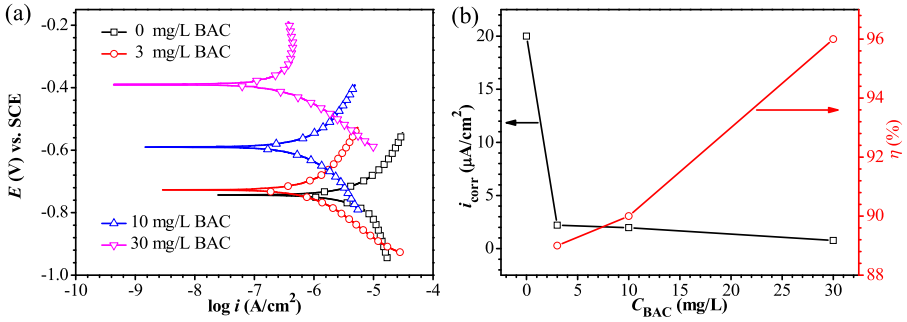

Fig. 7. Potentiodynamic polarization curves after 14 days of incubation in electrochemical glass cells for different BAC concentrations (a), corresponding i_{corr} values and i_{corr}-based inhibition efficiencies (b).

Without adequate suppression of algal growth, live cells of *C. vulgaris* produced oxygen via photosynthesis and this led to oxygen corrosion based on the following reactions [26,46]:

$$Fe \rightarrow Fe^{2+}+2e- \quad (2)$$

$$O_2+2H_2O+4e- \rightarrow 4OH- \quad (3)$$

$$Fe^{2+}+2OH- \rightarrow Fe(OH)_2 \quad (4)$$

The unstable $Fe(OH)_2$ was oxidized to $Fe(OH)_3/Fe_3O_4$. This sequence of reactions was the main reason for the severe MIC by *C. vulgaris*.

3.5. EIS

Nyquist and Bode plots during the 14 days of incubation with different BAC concentrations are shown in Fig. 6. An equivalent circuit model was used for fitting the EIS data and generating the fitted parameters (Fig. S2, Table S1). Overall, the diameters of the semi-circle of Nyquist plots increased with increasing BAC concentrations (Fig. 6(a–d)), suggesting increased corrosion inhibition by BAC because a larger diameter corresponded to a higher corrosion resistance. The fitted parameters indicate that charge transfer resistance (R_{ct}) dominated among all the resistances (transfer resistance, solution resistance and biofilm/corrosion product film resistance) (Table S1). It was found that 30 mg/L BAC greatly increased R_{ct} values.

3.6. Potentiodynamic polarization

Potentiodynamic polarization curves were obtained with and without BAC in the presence of *C. vulgaris*. Fig. 7(a) shows that current density (i) values for cathodic and anodic reactions decreased clearly in the presence of BAC, indicating effective inhibition. Fig. 7(b) shows the values of corresponding corrosion current density (i_{corr}) and inhibition efficiencies (η_i) obtained by fitting the potentiodynamic polarization curves (Table S3). In this work, to distinguish it from weight loss-based corrosion inhibition (η), η_i was used to denote the corrosion inhibition efficiency calculated from the following equation:

$$\eta_i(\%) = \frac{i^0_{corr} - i_{corr}}{i^0_{corr}} \times 100 \quad (5)$$

where i^0_{corr} and i_{corr} are the corrosion current densities in the absence and presence of BAC, respectively. Fig. 7(b) shows that i_{corr} decreased when BAC concentration increased, which led to increased η_i. At 30 mg/L, BAC achieved an η_i value of 96%, which was very close to the 95% weight-loss based corrosion inhibition efficiency.

Compared to the abiotic i_{corr} (Fig. S4 and Table S4), the i_{corr} in the presence of *C. vulgaris* was much larger, indicating acceleration of corrosion by the alga. BAC inhibited the corrosion by the abiotic culture medium (Table S4), but to a much less extent than in the inoculated culture medium. The abiotic η_i value for 30 mg/L was 73% vs. 96% for the biotic η_i. This indicated that the biocidal effect of BAC against the alga contributed to the overall corrosion inhibition efficiency considerably.

4. Conclusion

Algae have attracted attention in recent years because they can cause MIC. Hence, in this study, BAC inhibition of *C. vulgaris* MIC was studied. Results show that *C. vulgaris* grew well and consequently led to severe pitting and uniform corrosion. BAC was found to kill sessile *C. vulgaris* to a small extent at 3 mg/L, and to an undetectable extent outcome at 30 mg/L. BAC at 30 mg/L led to a high corrosion inhibition efficiency (95% based on weight loss or 96% based on i_{corr} reduction). This dosage is relatively low compared to typical biocide dosages of 50 mg/L and higher. The killing of *C. vulgaris* sessile cells and the adsorption of BAC molecules on the carbon steel both contributed to the overall corrosion inhibition efficiency.

Acknowledgements

This research was supported by National Key Research and Development Program of China (2018YFF0215002). Graduates' Innovation Fund of Huazhong University of Science and Technology (5003013044). The Open Fund of Hubei Key Laboratory of Materials Chemistry and Service Failure (2017), Key Laboratory of Materials Chemistry for Energy Conversion and Storage, Ministry of Education (2018). Natural Science Foundation of the Jiangsu Higher Education Institutions of China (No. 18KJB530004). JW thanks the China Scholarship Council for its support to study in USA. We also acknowledge the support of the Analytical and Testing Center of the Huazhong University of Science and Technology for SEM measurements.

Appendix A. Supplementary data

Supplementary material related to this article can be found, in the online version, at doi:https://doi.org/10.1016/j.jmst.2020.01.012.

References

[1] B.S. Hou, N. Xu, Q.H. Zhang, C.J. Xuan, H.F. Liu, G.A. Zhang, J. Taiwan Inst. Chem. Eng. 95 (2019) 541–554.
[2] R. Jia, D. Yang, D. Xu, T. Gu, Bioelectrochemistry 118 (2017) 38–46.
[3] H. Liu, Y.F. Cheng, Corros. Sci. 133 (2018) 178–189.
[4] Y. Li, Z. Wang, M. Zhao, G. Zhang, Ind. Eng. Chem. Res. 57 (2018) 8718–8728.
[5] Y. Li, D. Xu, C. Chen, X. Li, R. Jia, D. Zhang, W. Sand, F. Wang, T. Gu, J. Mater. Sci. Technol. 34 (2018) 1713–1718.
[6] J. Wang, B. Hou, J. Xiang, X. Chen, T. Gu, H. Liu, Corros. Sci. 150 (2019) 296–308.

[7] E. Heitz, W. Sand, H.-C.F (Eds.), Microbial Deterioration of Materials, Springer, 1996, p. 514.
[8] T. Gu, R. Jia, T. Unsal, D. Xu, J. Mater. Sci. Technol. 35 (2019) 631–636.
[9] Y. Huang, E. Zhou, C. Jiang, R. Jia, S. Liu, D. Xu, T. Gu, F. Wang, Electrochem. Commun. 94 (2018) 9–13.
[10] D. Xu, E. Zhou, Y. Zhao, H. Li, Z. Liu, D. Zhang, C. Yang, H. Lin, X. Li, K. Yang, J. Mater. Sci. Technol. 34 (2018) 1325–1336.
[11] E. Zhou, H. Li, C. Yang, J. Wang, D. Xu, D. Zhang, T. Gu, Int. Biodeterior. Biodegrad. 127 (2018) 1–9.
[12] J. Wang, C. Li, X. Zhang, M. Asif, T. Zhang, B. Hou, Y. Li, W. Xia, H. Wang, H. Liu, J. Electrochem. Soc. 166 (2019) G39–G46.
[13] J. Wang, F. Xiong, H. Liu, T. Zhang, Y. Li, C. Li, W. Xia, H. Wang, H. Liu, Bioelectrochemistry 129 (2019) 10–17.
[14] T. Wu, M. Yan, D. Zeng, J. Xu, C. Sun, C. Yu, W. Ke, J. Mater. Sci. Technol. 31 (2015) 413–422.
[15] M. Saleem Khan, Z. Li, K. Yang, D. Xu, C. Yang, D. Liu, Y. Lekbach, E. Zhou, P. Kalnaowakul, J. Mater. Sci. Technol. 35 (2019) 216–222.
[16] H. Li, C. Yang, E. Zhou, C. Yang, H. Feng, Z. Jiang, D. Xu, T. Gu, K. Yang, J. Mater. Sci. Technol. 33 (2017) 1596–1603.
[17] X. Shi, W. Yan, D. Xu, M. Yan, C. Yang, Y. Shan, K. Yang, J. Mater. Sci. Technol. 34 (2018) 2480–2491.
[18] M. Moradi, Z. Song, T. Xiao, J. Mater. Sci. Technol. 34 (2018) 2447–2457.
[19] Y. Dong, Y. Lekbach, Z. Li, D. Xu, S. El Abed, S.I. Koraichi, F. Wang, J. Mater. Sci. Technol. 37 (2020) 200–206.
[20] R. Jia, D. Yang, W. Dou, J. Liu, A. Zlotkin, S. Kumseranee, S. Punpruk, X. Li, T. Gu, Int. Biodeterior. Biodegrad. 139 (2019) 78–85.
[21] P. Li, Y. Zhao, Y. Liu, Y. Zhao, D. Xu, C. Yang, T. Zhang, T. Gu, K. Yang, J. Mater. Sci. Technol. 33 (2017) 723–727.
[22] H. Liu, T. Gu, G. Zhang, Y. Cheng, H. Wang, H. Liu, Corros. Sci. 102 (2016) 93–102.
[23] J. Xu, R. Jia, D. Yang, C. Sun, T. Gu, J. Mater. Sci. Technol. 35 (2019) 109–117.
[24] Q. Qu, S. Li, L. Li, L. Zuo, X. Ran, Y. Qu, B. Zhu, Corros. Sci. 118 (2017) 12–23.
[25] E. Khamis, E. El-Rafey, A. Moustafa Abdel Gaber, A. Hefnawy, N. Galal El-Din Shams El-Din, M. Salah El-Din Esmail Ahmed, Desalin. Water Treat. 57 (2016) 23571–23588.
[26] H. Liu, D. Xu, A.Q. Dao, G. Zhang, Y. Lv, H. Liu, Corros. Sci. 101 (2015) 84–93.
[27] X. He, Y.-L. Liu, A. Conklin, J. Westrick, L.K. Weavers, D.D. Dionysiou, J.J. Lenhart, P.J. Mouser, D. Szlag, H.W. Walker, Harmful Algae 54 (2016) 174–193.
[28] M.A. Mallin, M.R. McIver, E.J. Wambach, A.R. Robuck, Lake Reserv. Manage. 32 (2016) 168–181.
[29] B. Ma, Y. Chen, H. Hao, M. Wu, B. Wang, H. Lv, G. Zhang, Colloids Surf. B Biointerfaces 41 (2005) 197–201.
[30] Q. Liao, H.-X. Chang, Q. Fu, Y. Huang, A. Xia, X. Zhu, N. Zhong, Bioresour. Technol. 250 (2018) 583–590.
[31] Y. Sun, Q. Liao, Y. Huang, A. Xia, Q. Fu, X. Zhu, J. Fu, J. Li, Bioresour. Technol. 256 (2018) 421–430.
[32] H. Liu, M. Sharma, J. Wang, Y.F. Cheng, H. Liu, Int. Biodeterior. Biodegrad. 129 (2018) 209–216.
[33] M. Kim, J.K. Hatt, M.R. Weigand, R. Krishnan, S.G. Pavlostathis, K.T. Konstantinidis, Appl. Environ. Microbiol. 84 (2018) e00197–00118.
[34] S.M. Choi, T.H. Roh, D.S. Lim, S. Kacew, H.S. Kim, B.-M. Lee, J. Toxicol. Environ. Health, Part B 21 (2018) 8–23.
[35] Y. Zhu, M.L. Free, G. Yi, Corros. Sci. 102 (2016) 233–250.
[36] Y. Zhu, M.L. Free, Colloids Surf. Physicochem. Eng. Asp. 489 (2016) 407–422.
[37] L. Guo, S. Zhu, S. Zhang, J. Ind. Eng. Chem. 24 (2015) 174–180.
[38] Y. Zhu, M.L. Free, G. Yi, J. Electrochem. Soc. 162 (2015) C582–C591.
[39] H. Liu, T. Gu, Y. Lv, M. Asif, F. Xiong, G. Zhang, H. Liu, Corros. Sci. 117 (2017) 24–34.
[40] G. ASTM Standard Practice for Preparing, Cleaning, and Evaluating Corrosion Test Specimens," Philadelphia, Pennsylvania: Am. Soc. Test. Mater., 2003.
[41] N.K. Gupta, C. Verma, M.A. Quraishi, A.K. Mukherjee, J. Mol. Liq. 215 (2016) 47–57.
[42] Y. Qiang, S. Zhang, S. Xu, W. Li, J. Colloid Interface Sci. 472 (2016) 52–59.
[43] M.J. Hernández Gayosso, G. Zavala Olivares, N. Ruiz Ordaz, C. Juárez Ramirez, R. Garc'ıa Esquivel, A. Padilla Viveros, Electrochim. Acta 49 (2004) 4295–4301.
[44] Y. Han, J. Wang, H. Zhang, S. Zhao, Q. Ma, Z. Wang, Sens. Actuators 250 (2016) 78–86.
[45] A.B. Ikhe, A.B. Kale, J. Jeong, M.J. Reece, S.-H. Choi, M. Pyo, Corros. Sci. 109 (2016) 238–245.
[46] H. Liu, T. Gu, M. Asif, G. Zhang, H. Liu, Corros. Sci. 114 (2017) 102–111.